

Electrical Characterization of Semi-insulating Devices for Electrophotography

*Inan Chen and Ming-Kai Tse
QEA, Inc.*

755 Middlesex Turnpike, Unit 3, Billerica MA 01821 USA

Tel: (978) 528-2034 · Fax: (978) 528-2033

e-mail: info@qea.com

URL: www.qea.com

*Paper presented at the IS&T's NIP15
International Conference on Digital Printing Technologies
Oct 17-22, 1999, Orlando, Florida*

Electrical Characterization of Semi-insulating Devices for Electrophotography

Inan Chen and Ming-Kai Tse
QEA, Inc.
Burlington, Massachusetts, USA

Abstract

It has been shown that in semi-insulating films, the characterization of charge transport phenomena, such as dielectric relaxation, by resistance and capacitance only is insufficient. The independent roles played by additional transport parameters, including charge injection, trapping and field dependent mobility, are elucidated by a first principle treatment of charge transports in both the closed circuit and open circuit modes. Experimental results from typical electrophotographic paper and charging roll samples are compared with the results of mathematical simulations. The advantage of open circuit measurements, such as Electrostatic Charge Decay (ECD), is noted.

Introduction

Polymeric semi-insulating composite materials are widely used in electrophotography for charging rolls, developer rolls, transfer media, and charge transport layers. The performance of these components depends critically on the dielectric relaxation during the process. It is commonly understood that dielectric relaxation is related to the resistivity of the material, and the resistivity is determined by current-voltage measurements assuming Ohmic conduction. However, the inhomogeneity and low purity of the composite materials can be expected to introduce special features such as non-Ohmic injection, trappings and field dependent mobility. Thus, a question arises as to whether the traditional treatment of dielectric relaxation by equivalent circuit, specifying a sample by its resistance and capacitance only, is adequate for these devices. In fact, experimental data have shown that the relaxation does not always follow the exponential time dependence predicted by the equivalent circuit model.¹

In this paper, the independent roles played by various transport parameters, including charge injection, trapping and field dependent mobility, are elucidated by a first principle treatment of charge transports in both the closed circuit and open circuit modes. Experimental results from typical electrophotographic paper and charging roll samples are compared with the results of mathematical simulations.

It is concluded that because the measurements are carried out under conditions closely simulating the actual application of the device, open circuit measurements, such as the Electrostatic Charge Decay (ECD) technique,² can

provide more relevant information on the performance of the device than the closed circuit mode of measurements.

Charge Transport Equations

Consider the two configurations for electrical characterization of semi-insulating films. In the closed circuit mode schematically shown in Fig. 1(A), a constant voltage V_0 is applied across the sample, and the total current J_T in the external circuit is measured. In the open circuit mode shown in Fig. 1(B), the surface of a grounded sample is charged (e.g. with corona ions) to a given voltage V_0 , and the decay of the voltage is measured as a function of time.

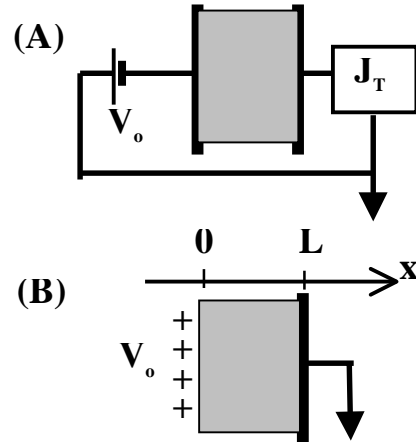


Figure 1. Schematics of (A) closed circuit mode and (B) open circuit mode measurements.

The mathematical simulation of these two measurements starts with the expression of the time-dependent total current J_T as the sum of conduction and displacement currents,

$$J_T(t) = (\mu_p q_p + \mu_n q_n)E + \varepsilon(\partial E/\partial t) \quad (1)$$

where q and μ denote the charge density and drift mobility, respectively, with the subscripts p and n referring to holes and electrons, respectively. ε is the permittivity of the sample. Noting that the integral of field E over the sample thickness L gives the voltage across the sample V , an integration of Eq.(1) yields,

$$J_T(t) = [\int_0^L (\mu_p q_p + \mu_n q_n)Edx - \varepsilon(dV/dt)]/L \quad (2)$$

In the closed circuit mode of Fig. 1(A), the second term in Eq.(2) vanishes because the voltage remains constant. Thus, the total current in Eq.(2) reduces to,

$$J_T(t) = \left[\int_0^L (\mu_p q_p + \mu_n q_n) E dx \right] / L \quad (3)$$

In the open circuit mode of Fig. 1(B), the total current is zero. Thus, the voltage is given by the integral of its time derivative from Eq.(2),

$$dV/dt = \left[\int_0^L (\mu_p q_p + \mu_n q_n) E dx \right] / \epsilon \quad (4)$$

The time dependence of local charge density $q_p(x,t)$, and $q_n(x,t)$, is determined by the continuity equations:

$$\partial q_p / \partial t = \partial (\mu_p q_p E) / \partial x - q_p / \tau_p \quad (5a)$$

$$\partial q_n / \partial t = \partial (\mu_n q_n E) / \partial x - q_n / \tau_n \quad (5b)$$

where τ_p and τ_n are the lifetime to deep trapping for holes and electrons, respectively. The density of deep trapped charge $q_t(x,t)$ increases with time as,

$$\partial q_t / \partial t = q_p / \tau_p + q_n / \tau_n \quad (6)$$

The field $E(x,t)$ is related to the charge densities by the Poisson equation,

$$\partial E(x) / \partial x = (q_p + q_n + q_t) / \epsilon \quad (7)$$

The drift mobility can be field dependent. For lack of better knowledge, it is assumed to have the following power-law dependence, with μ_{p0} and μ_{n0} denoting the mobilities at a nominal field E_0 :

$$\mu_p(E) = \mu_{p0} (E/E_0)^m ; \mu_n(E) = \mu_{n0} (E/E_0)^m \quad (8)$$

where the power m may not be the same for holes and electrons.

At the boundaries, $x=0$ and L , the charge injections into the sample can be specified by assuming the injection currents $J_p(0, t)$ and $J_n(L, t)$ to be proportional to the fields at the boundaries,

$$J_p(0, t) = s_p E(0, t) ; J_n(L, t) = s_n E(L, t) \quad (9)$$

Note that the proportionality constants s_p and s_n have the dimension of conductivity.

From a given set of initial and boundary conditions, the above equations can be solved by numerical iteration to simulate the experimentally observed currents or voltages, Eqs. (3) or (4). Examples of the numerical results are presented and discussed in the following sections. In these figures, unless otherwise stated, the mobilities are assumed to be field independent, having the same values in all samples, and are equal for holes and electrons. The common mobility μ_0 is used to define the nominal transit time $t_0 \equiv L^2 / \mu_0 V_0$ as the unit of time.

Closed Circuit Mode

In Fig. 2, the intrinsic charge densities, $q_i = \sigma / (\mu_p + \mu_n)$, of the three samples differ by two orders of magnitude, and have the values 0.1, 1 and 10 (in units of $q_0 \equiv \epsilon V_0 / L^2$). Two different injections are considered for each of the three samples. The injection parameters of the highly injecting

case (solid curves) are $s_p = s_n = 10$, and those of the weakly injecting case (dashed curves) are $s_p = s_n = 0.1$ (in units of $\sigma_0 \equiv \mu_0 q_0 = \epsilon \mu_0 V_0 / L^2$). The injections of holes and electrons from the anode and cathode, respectively, are assumed to be symmetric.

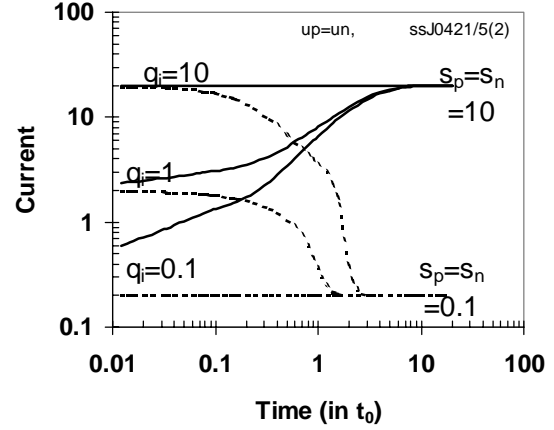


Figure 2. Current vs. time for three samples of different intrinsic charge densities q_i with two different injection levels $s_p (=s_n)$.

It can be seen from this figure that the currents at short times, $t < t_0$ are determined by the intrinsic charge density q_i (or the conductivity). On the other hand, the steady state currents, which are reached in about $10t_0$, are determined by the injection levels s_p and s_n .

Calculations have been repeated for asymmetric injections, $s_p \neq s_n$, to show that the above features are independent of the assumption of symmetric injection.

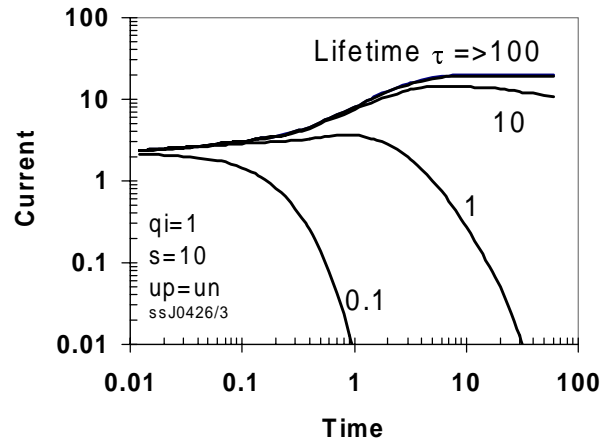


Figure 3. Current vs. time for samples with different lifetime to deep trapping τ .

In the conventional resistance measurements, the resistance is determined from the applied voltage and the steady state current. Then, the above findings indicate that such a resistance value would be strongly dependent on the

injection levels from the electrodes, but have little relation to the intrinsic conductivity.

In Fig. 3, the deep trapping of charge with a lifetime τ shorter than $10t_0$ is shown to reduce the current so significantly that no steady state currents can be measured. On the other hand, the curves in Fig. 4 illustrate that the field dependence of mobility has little effect on the current characteristics. This can be understood, as the field remains almost constant across the sample throughout the current flow in the closed circuit mode. This is not the case for the open circuit mode to be discussed next.

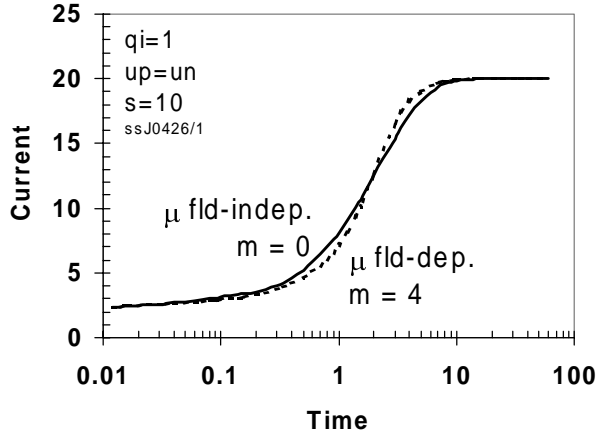


Figure 4. Current vs. time for samples with field independent and field dependent mobilities

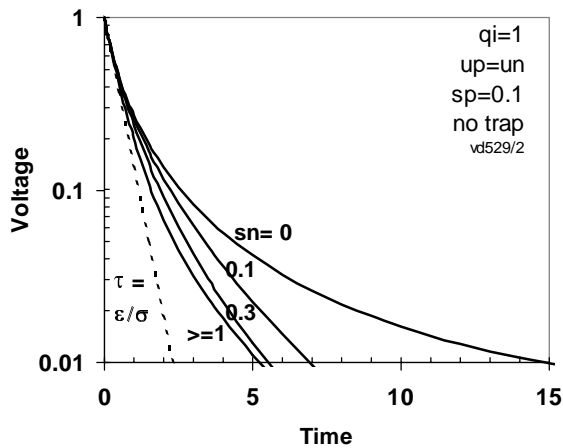


Figure 5. Voltage decay of samples with asymmetric injections

Open Circuit Mode

In the open circuit mode, it is most likely that the injections from the two boundaries are not equal. In Fig. 5, the voltage decay curves are shown for the cases where the injection from the surface is weak, with a fixed value of $s_p = 0.1\sigma_0$, while the injection from the substrate s_n is varied. The voltage decay is seen to be slower than the exponential one

with a time constant $\tau = \epsilon/\sigma$, expected from the equivalent circuit model, in spite of how large s_n is.

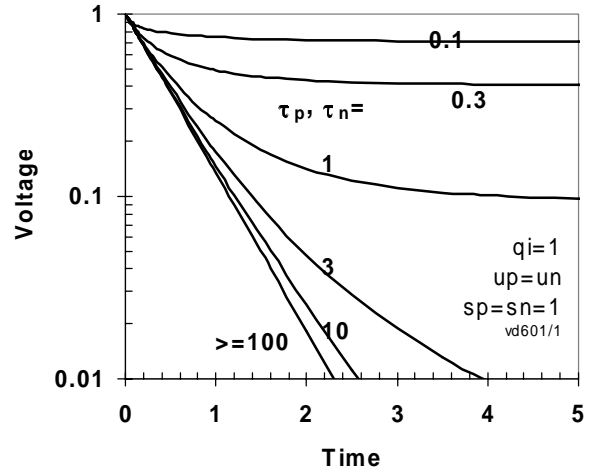


Figure 6. Voltage decay of samples with different life time to deep trapping $\tau_p (= \tau_n)$.

The loss of mobile charge due to deep trapping, i.e. short lifetimes τ_p, τ_n , leads to further slowing down of voltage decay as illustrated in Fig. 6. Even for an injection level ($s_p = s_n \geq 1$) that gives an exponential decay when the lifetime is long, $\tau_p, \tau_n > 100t_0$ the decay deviates significantly from the exponential form for $\tau_p, \tau_n < 10t_0$.

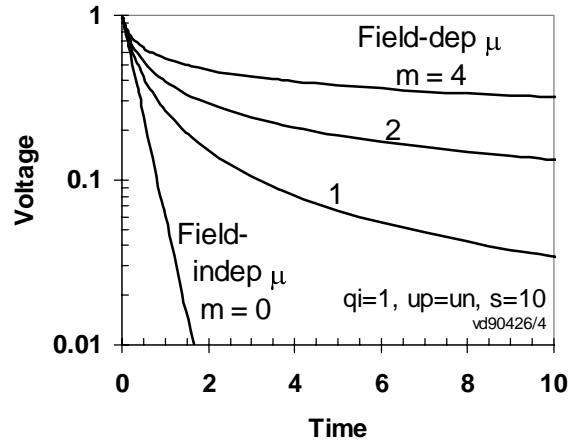


Figure 7. Voltage decay of samples with different field dependence of mobilities

The consequences of field dependent mobility are illustrated in Fig. 7. Both hole and electron mobilities are assumed to follow the power law, Eq.(8). It can be seen that as the power m increases from zero (field independent) to 4, the decay slows down and deviates from the exponential form. In contrast to the current in closed circuit mode (Fig. 4), the pronounced sensitivity of voltage decay to field dependence can be expected because the fields change (decrease) significantly throughout the decay.

Experimental Results

It has been demonstrated that dielectric relaxation in the thin semi-insulative coating (outside the conductive elastomer) of the charging rolls plays an important role in the performance of the device.^{1,2} Similarly in electrostatic transfer, dielectric relaxation of the transfer media (e.g. paper) has been shown to have an important influence on the transfer efficiency.³

An open circuit mode of measurement – the electrostatic charge decay (ECD) technique – has been developed for efficient evaluations of various semi-insulating devices in electrophotography.² Two examples of the data from charging rolls (CR-1 and CR-2) and from electrophotographic paper samples (PP-1 and PP-2) are shown in Fig. 8. The open surface is corona charged and the decay of surface voltage is measured as a function of time. The paper samples are wrapped around a grounded metal shaft.

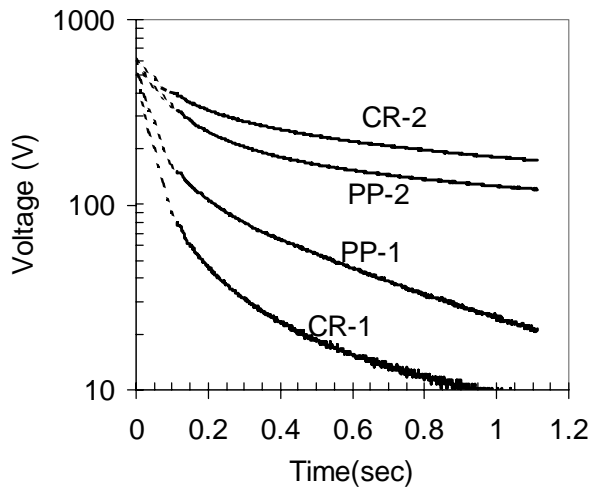


Figure 8. Electrostatic charge decay (ECD) curves of charging rolls (CR-1, -2) and paper samples (PP-1, -2)

Because of the spatial separation between the corotron and the voltage probe, a short delay exists between the charging time and the beginning of voltage measurements. By extrapolating the decay curves (as shown by the dashed curves), the initial voltages can be estimated to be several hundred V. The thickness of the semi-insulating layers is about 10^{-2} cm. If the mobility is of the order of 10^{-6} cm^2/Vsec , the nominal transit time (used as the time units in the simulated curves in the previous sections) is $t_0 \approx 0.1$ sec. Thus, the time axis in Fig. 8 covers the time range approximately from $t = 0$ to $12 t_0$.

Discussion

All four voltage decay curves in Fig. 8 are seen to be not exponential. Comparing these curves with the simulated curves of Fig. 5, one could attribute this non-exponential decay to the unequal charge injections at the corona charged surface and at the conductive (metal) shaft. However, a more quantitative comparison (using the above t_0 value)

reveals that the decay is slower than that seen in Fig. 5. This suggests that either deep trapping (Fig. 6) or field dependent mobility (Fig. 7), or both, must be in effect. From the fact that finite steady state currents are observed in these samples in the closed circuit measurements, the lifetime should not be shorter than $100t_0$ (cf. Fig. 3). Thus, we conclude that charge mobility is strongly field-dependent, and this causes the slow voltage decay, or dielectric relaxation, in these semi-insulator layers. From a semi-quantitative comparison of Figs. 7 and 8, one can estimate the field dependence power to be $m \approx 1$ for the samples CR-1 and PP-1, and $m > \approx 2$ for CR-2 and PP-2.

It should be emphasized that this field-dependence of mobility is revealed by the open circuit measurements of ECD technique conveniently in a single decay curve. In contrast, the closed circuit, steady state current is not sensitive to field dependence (as shown in Fig. 4). To detect field dependence, measurements have to be repeated with different applied voltages.

In many electrophotographic sub-processes, e.g. in electrostatic transfer or roller charging, although a constant bias is applied across the multiple layers, the voltage across the semi-insulating layer (e.g. paper or roller coating), decreases with time, as if in an open-circuit mode. Therefore, the field dependence of the transport parameters, such as mobility and lifetime, plays an important role in the actual processes.

The fact that open circuit mode measurements, such as ECD,² can simulate the field conditions in actual processes and reveal the consequences of field dependence, is an important merit of the ECD technique over other measurement techniques using the constant voltage, closed circuit mode.

References

1. M. K. Tse and I. Chen, The role of dielectric relaxation in charge roller performance, Proc. NIP14, pg. 481 (1998)
2. M. K. Tse, D. J. Forest, and F. Y. Wong, Predicting charge roller performance in electrophotography using electrostatic charge decay measurements, Proc. NIP11, pg.383 (1995)
3. I. Chen and M. K. Tse, The role of dielectric relaxation in media for electrophotography, (I) Modeling of electrostatic transfer, Proc.. NIP 15 (this issue, 1999)

Biography

Inan Chen received his Ph.D. from the University of Michigan in 1964. After a year of post-doctoral research there, he joined Xerox Research Laboratories in 1965 and retired in 1998. Currently he is associated with QEA, Inc. as a consulting research scientist. He has (co)authored over 100 publications, including eight US patents, in the fields of materials, devices and processes related to electrophotography. E-mail: inanchen@aol.com or mkt@qea.com.